Analysis of MRS Spectrum and Shannon Entropy Changes Under the Influence of the Faradarmani Consciousness Field (Task) and without it (Rest)

Mohammad Ali Taheri[1], Sara Torabi[2], Farid Semsarha[3*]

1. Sciencefact R&D Department, Cosmointel Inc. Research Center, Ontario, Canada
2. Department of Plant Biology, School of Biology, College of sciences, University of Tehran, Tehran, Iran
3.Institute of Biochemistry and Biophysics (IBB), University of Tehran, Tehran, Iran

* Corresponding author: Farid Semsarha
Email: Semsarha@ut.ac.ir

DOI: https://doi.org/10.61450/joci.v5i20.232

Abstract

The Faradarmani Consciousness Field is non-physical in nature, and its influence begins through the human mind. In a previous study using fMRI, it was shown that specific brain regions in trained individuals, known as Faradarmangars, became activated or deactivated during the task state involving the use of this field. Proton magnetic resonance spectroscopy (^{1}H-MRS), as a non-invasive method, allows for the assessment of changes in brain function and metabolism during exposure to the Faradarmani Consciousness Field. In this study, changes in the output spectrum from the MRS method were analyzed without focusing on any specific metabolite, accompanied by the calculation of Shannon entropy based on the distribution of spectral values. In fact, through this analysis, prior to the detailed examination of each individual metabolite, we gain insight into possible overall metabolic changes in the brains of Faradarmangars based on the obtained spectrum. This research significantly contributes to understanding general metabolic changes involved in brain activation and deactivation, as well as identifying the contrast between activated and deactivated areas based on the quantitative metric of entropy. According to the results of this study, the MRS spectrum showed an approximately 30% overall reduction in amplitude in the brain's activation region and about a 20% decrease in the Shannon entropy of amplitude distribution in comparison to the average control group. In contrast, no significant changes were observed in these parameters in the deactivated region.

Keywords: MRS, metabolite, spectrum, Shannon entropy, amplitude, Faradarmani

Introduction

Magnetic resonance (MR) imaging, introduced in the 1980s, has revolutionized the diagnostic landscape of central nervous system (CNS) disorders (Oz et al., 2014). Over the past few decades, MR techniques have continued to evolve, giving rise to advanced methods such as functional MRI (fMRI), and proton magnetic resonance spectroscopy (^{1}H-MRS), which have further enhanced our understanding of brain function, metabolism, and pathology (Padelli et al., 2022). Instead of displaying visual images of structures, MRS generates a linear spectrum — a graph with chemical shift (in parts per million, ppm) on the x-axis and signal intensity (amplitude) on the y-axis. Each peak in the spectrum corresponds to a specific metabolite, allowing researchers to identify and quantify brain metabolites such as N-acetylaspartate (NAA), choline (Cho), creatine (Cr), and others (Liserre et al., 2021).

The concept of Shannon entropy has so far been used to analyze large datasets obtained from biological samples. In biology, Shannon entropy is commonly applied to measure diversity and to determine the distribution and interactions of cells, genes, or molecules (Roach, 2020). Initially, Shannon entropy was used to represent the randomness in DNA sequences composed of the four nucleotides: adenine (A), cytosine (C), guanine (G), and thymine (T) (Schmitt and Herzel, 1997; Li et al., 2019). In systems biology, information content is described using Shannon entropy (Uda, 2020), and it has been applied to evaluate the robustness of signal transmission across various omics layers, such as transcriptomics, proteomics, and metabolomics (Uda et al., 2013).

For example, Shannon entropy calculated from mass spectrometry data of peanuts was used to identify advanced glycation end-products (Johnson et al., 2016). The application of Shannon entropy to RNA-seq datasets has also proven valuable for rapid and in-depth analysis of gene expression changes (Zambelli et al., 2018). In another case, antibodies in human blood were identified using a peptide microarray, and Shannon entropy calculated from the resulting profiles was proposed as an indicator of individual and population health status (Wang et al., 2017).

Based on Taheri's theory, there are various T-Consciousness Fields (TCFs), which are subcategories of the Cosmic Consciousness Network (CCN). The Faradarmani Consciousness Field is one of these non-physical fields. In this approach, these fields can be utilized by humans. Indeed, information transmitted from TCFs can induce alterations in the subject under study (Taheri, 2013).

As cited in the references, all metabolite-related data are derived from the output spectrum of the MRS method. In this study, prior to conventional spectral analyses and the extraction of data on the concentration and types of individual metabolites, we conducted a direct and independent examination of the raw MRS output spectrum, analyzing it using Shannon entropy. Previously, multiple studies involving T-Consciousness Fields have also measured Shannon entropy and analyzed the effects of such fields on the subject under investigation (Taheri et al., 2022a).

Method

MRI was performed on a 3.0-T clinical scanner (Magnetom Prisma, Siemens Medical Solutions, Erlangen, Germany) with a gradient strength of 40 mT/m. A body-connected coil enabled the transmission of excitation. Specifically, a ^{1}H phased-array head coil (125 MHz) was used for signal detection (Siemens Rapid Biomedical, Germany).

After acquiring scout images of the subjects, a T2-weighted imaging protocol was performed in axial and coronal planes to capture data from the regions of interest. The MRI protocols were also followed for the MRS experiments. Data acquisition was conducted in two phases: similarly to previous steps, from baseline up to 15 minutes before the onset of treatment (rest phase), and immediately after the initiation of the treatment up to 15 minutes (task phase).

The T2-weighted imaging protocol was based on a standard spin-echo sequence with the following parameters: TR/TE = 5000/77 ms, NEX = 2, FOV = 4 × 4 cm^2, matrix size = 256 × 256, and slice thickness = 1 mm. Prior to performing MRS, a voxel of 1×1×1 cm^3 was defined in each of the three target regions for each subject. Following manual shimming and water suppression adjustment, short-echo proton MR spectra with high signal quality were acquired using the PRESS technique (TR/TE=6000/135 ms, 156 acquisitions).

Before starting the MRS test, water suppression was performed using second-order shimming and a Chemical Shift Selective (CHESS) pulse sequence. At the end of the MRS experiment, the reference water signal was acquired by disabling water suppression to allow for metabolite concentration calibration. The described MRI and MRS protocols were conducted similarly both before and after the treatment process. Rest and task imaging were performed sequentially without moving the subjects and with their eyes completely closed during both phases.

Experimental design

Based on fMRI data from previous studies, in order to investigate metabolic changes in the activated and deactivated brain regions of Faradarmangars, three regions were selected: one containing an activated area (right Precentral Gyrus), one containing a deactivated area (right Superior Temporal Gyrus), and a third region with similar dimensions located between the activated and deactivated areas, which, according to the obtained data (Taheri et al., 2022b), does not show activation or deactivation in response to the Faradarmani Consciousness Field (Figure 1). The third region was chosen to serve as a negative control for comparing potential metabolic changes with the other two regions. Images of the selected regions and the MRS spectra obtained during the rest state are presented in Figures 2 to 4.

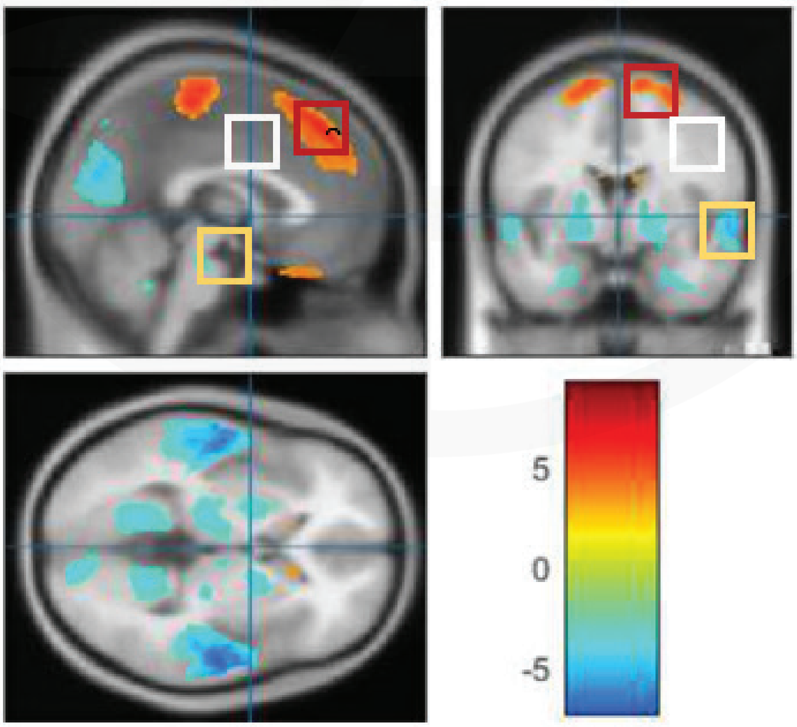

Figure1. Three selected regions based on fMRI data. Red box: Activated region, Yellow box: Deactivated region, White box: Neither activated nor deactivated region (Taheri et al., 2022b).

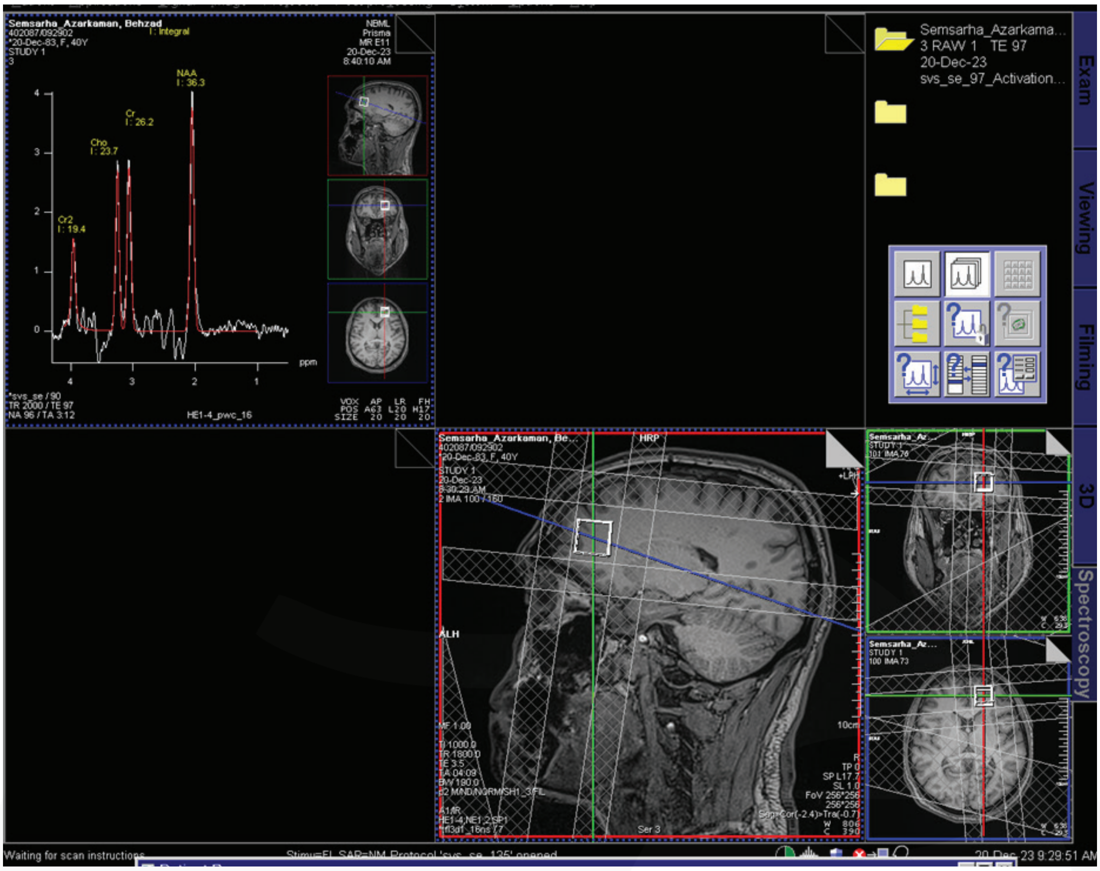

Figure 2. T2-weighted MR image of one of the study subjects, showing the placement of the MRS voxel on the selected activated region under Faradarmani Consciousness Field treatment, along with the proton spectrum obtained in the rest state.

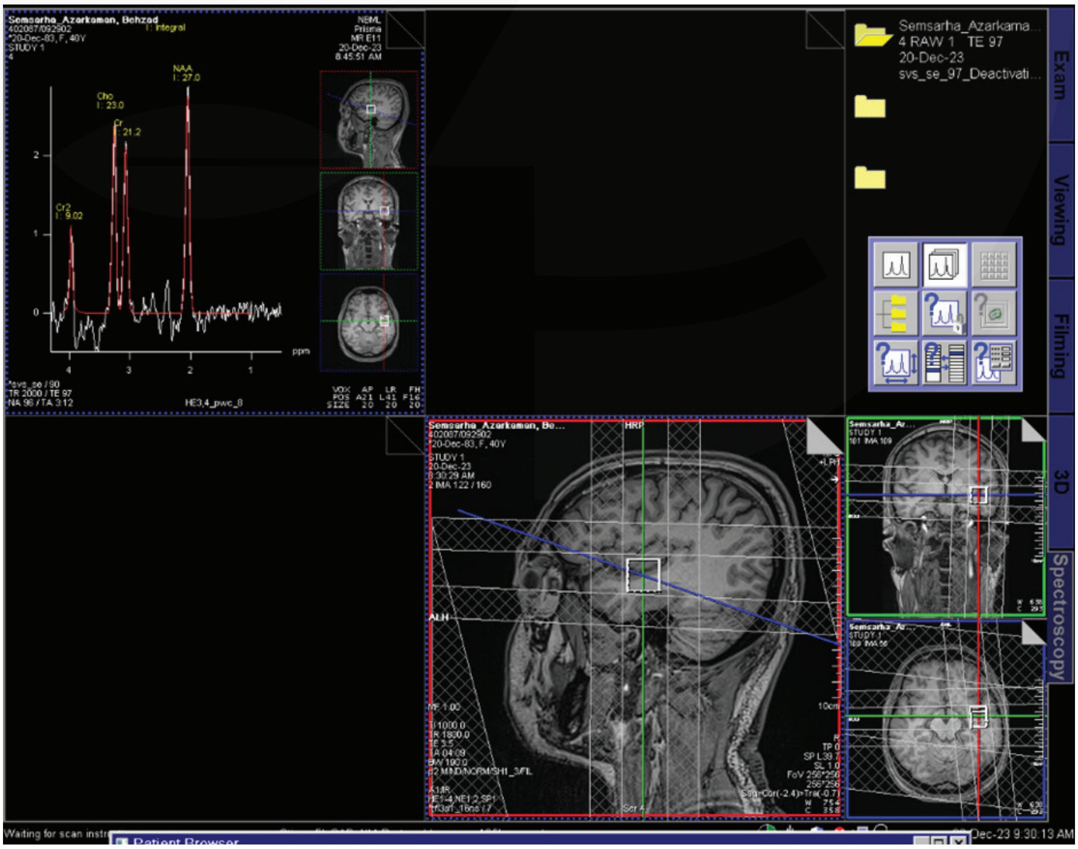

Figure 3. T2-weighted MR image of one of the study subjects, showing the placement of the MRS voxel on the selected deactivated region under Faradarmani Consciousness Field treatment, along with the proton spectrum obtained in the rest state.

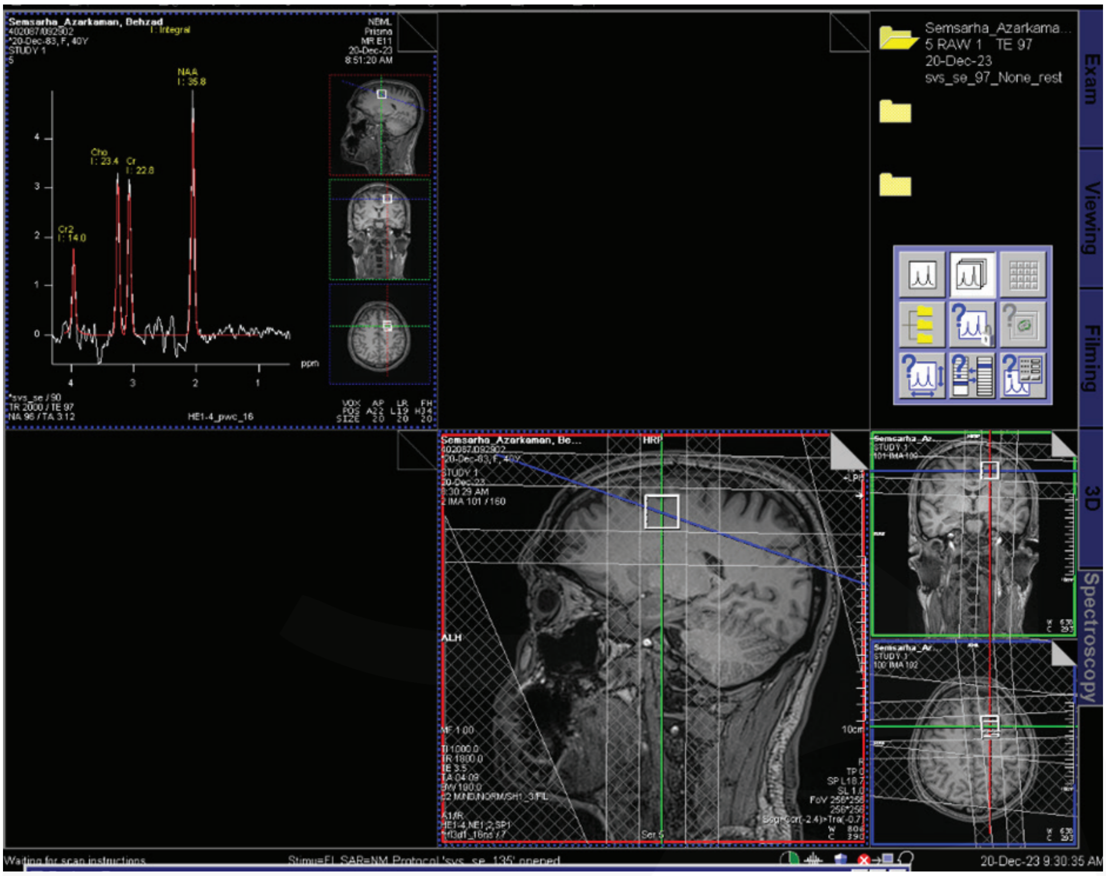

Figure 4. T2-weighted MR image of one of the study subjects, showing the placement of the MRS voxel on the selected neither activated nor deactivated region during Faradarmani Consciousness Field treatment, along with the proton spectrum obtained in the rest state.

Analysis of the MR spectrum

The volume of interest (VOI) for the MRS experiments was drawn on T2-weighted images. We attempted to create identical VOIs for the three regions across different subjects to ensure similar coverage of the target areas in each individual. Each spectrum corresponding to the selected regions was analyzed using a Java-based graphical user interface. This interface, used for the MRUI quantification package, contains a basic knowledge base of 57 peaks associated with at least 34 different metabolites. Metabolite concentrations were determined relative to the water signal used as a reference. Therefore, all amplitudes in each MR spectrum were expressed semi-quantitatively. It is also worth mentioning that the advanced method for accurate, robust, and efficient spectral fitting (AMARES) was used for quantification (Vanhamme et al., 1997).

The Application of Faradarmani Consciousness Field

In the present study, a population-level MRS analysis was conducted on Faradarmangars, comparing metabolite changes in selected brain regions during the task and rest phases. The task refers to the activity during which a Faradarmangar personally connects to the Cosmic Consciousness Network. This study was approved by the Ethics Committee of Iran University of Medical Sciences (Approval ID: IR.IUMS.REC.1402.940).

Thirty healthy adult participants (mean age: 42 ± 7 years), all with no history of neurological or psychiatric medication use in the six months prior to the test day, were included in the study group. Of these participants, 40% were male (n = 12) and 60% were female (n = 18). The design of the studies conducted using the MRS technique included a 15-minute rest phase (prior to connection with the field) and a 15-minute task phase, representing the state of connection with the Faradarmani Consciousness Field (initiated immediately after the rest phase). Further details about each phase of the study in chronological order are as follows:

1. **Rest**: A 15-minute initial phase in which Faradarmangars were instructed, while inside the MRI scanner, to keep their eyes closed and remain relaxed and stress-free, without engaging with any Consciousness Fields. The purpose of this phase was to obtain control data, representing the baseline state before connection with the field. This baseline plays a critical role in constructing population-level control data or "pre-connection" references.

2. **Task**: In this study, the second 15-minute phase—immediately following the rest phase without any temporal gap—is referred to as the task phase. In this phase, the individuals establish a connection with the Faradarmani Consciousness Field. This connection is initiated solely by the participants themselves upon hearing a predefined beep, which they had been informed in advance signals the beginning of the connection.

3. Data Analysis

The data obtained from this study were statistically analyzed using GraphPad software (version 9). One-way analysis of variance (ANOVA) was used to assess metabolite levels in comparisons between control and test samples. For the MRS datasets of each group, the Wilcoxon test was applied at a 5% significance level to compare changes in the concentration of each metabolite before and after treatment with the Faradarmani Consciousness Field.

Results and Discussion

In this study, without performing separate analyses of individual metabolites or focusing on their specific details, the overall MRS spectra were compared and examined. Figure 5 shows the spectral changes during the task state under the influence of the Faradarmani Consciousness Field, relative to the rest state, in activated and deactivated brain regions of the Faradarmangars.

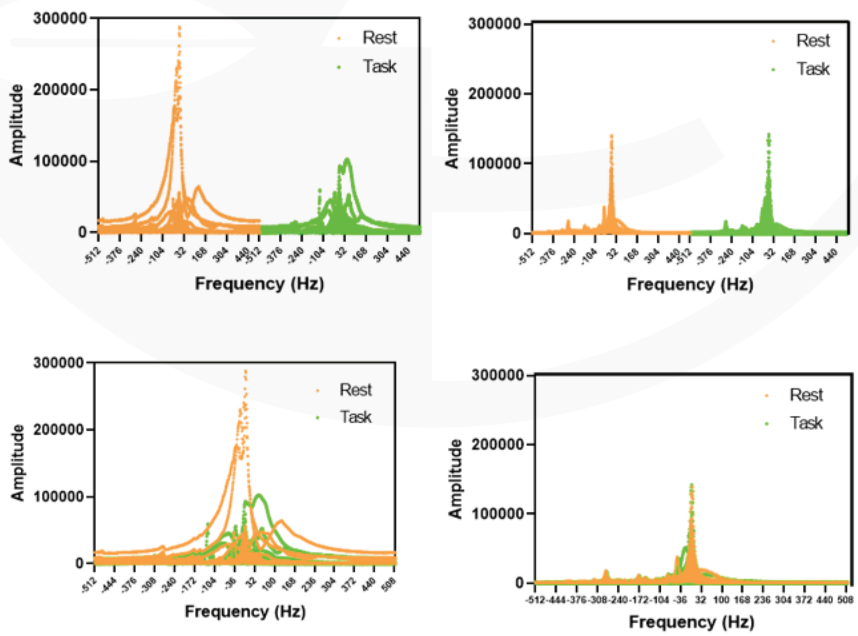

Figure 5. Comparison of the obtained spectra during the first 15 minutes (rest) and the second 15 minutes (task), shown separately (top) and overlaid (bottom). The task state refers to the condition under the influence of the Faradarmani Consciousness Field, while the rest state refers to the condition without it. Right: deactivated brain regions; Left: activated brain regions.

As shown in Figure 5, in the activated brain regions, the task state exhibits a reduction in the area under the peaks as well as a decrease in the peak power of the dominant signals. In contrast, in the deactivated regions, the task and rest spectra show a high degree of alignment despite existing differences. For improved comparison, the averaged peaks of the samples have also been compared, presented in Figures 6 and 7 and Table 1.

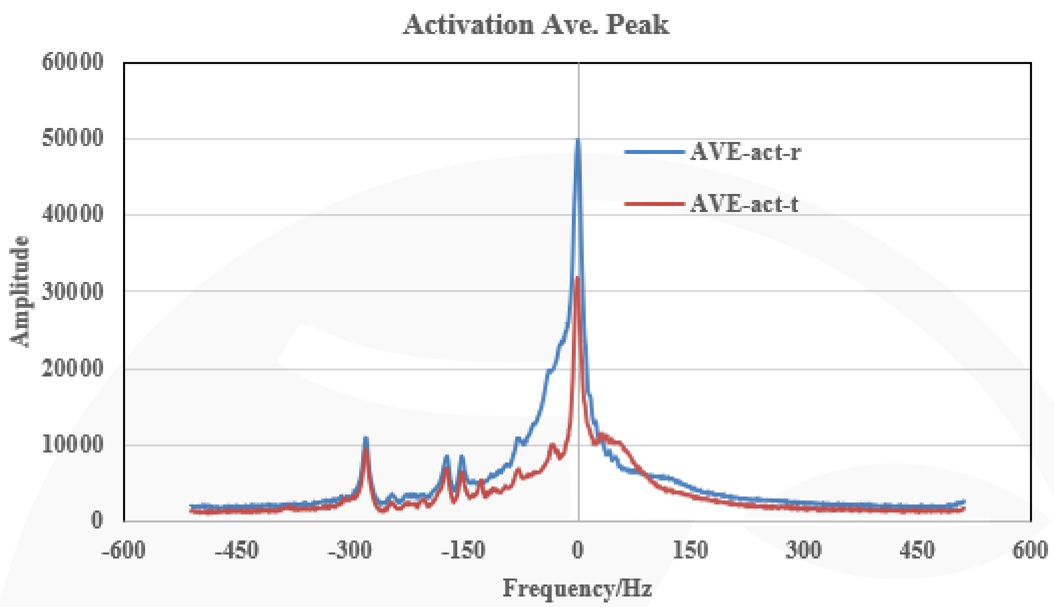

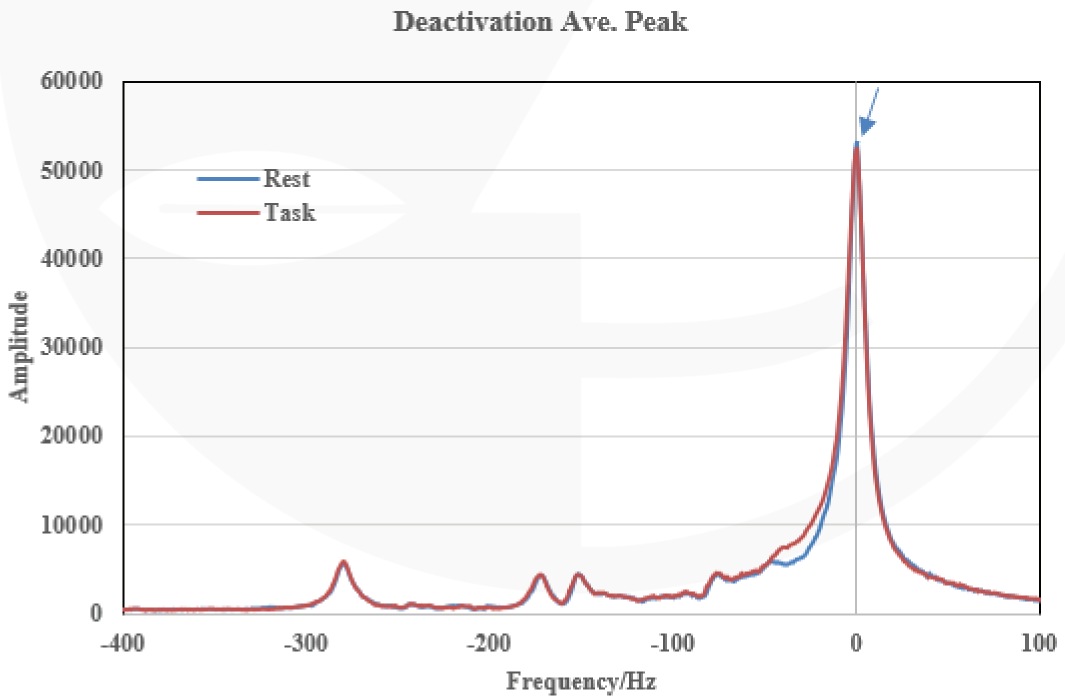

Figure 6. Comparison of the averaged spectra in the task and rest states in the activated brain region (top) and the deactivated brain region (bottom). The task state refers to the condition with exposure to the Faradarmani Consciousness Field, and the rest state refers to the condition without it. Red arrows indicate amplitude increases resulting from the task state, while blue arrows indicate amplitude increases resulting from the rest state.

Table 1. Comparison of the averaged spectra in the activated and deactivated brain regions of the Faradarmangars in the rest state (without Faradarmani Consciousness Field) and the task state (with Faradarmani Consciousness Field).

	Activation		**Deactivation**	
	Rest	Task	Rest	Task
Total Peak Area	5414030	3781657	2334550	2343484
Std. Error	348326	173718	92973	96046
Peak Y	49887	31836	52588	49905
Area	5414030	3781657	2334550	2343484
Std. Error	348326	173718	92973	96046

As shown in Figures 6, 7, and Table 1, the spectrum of the activated brain region of Faradarmangars exhibits a significant difference between task and rest, with a decrease observed during the task. This difference in the area under the peak shows a reduction of approximately 30% in the task state compared to the rest state. However, no significant difference is observed between task and rest in the deactivated brain region of Faradarmangars (less than 0.5% difference).

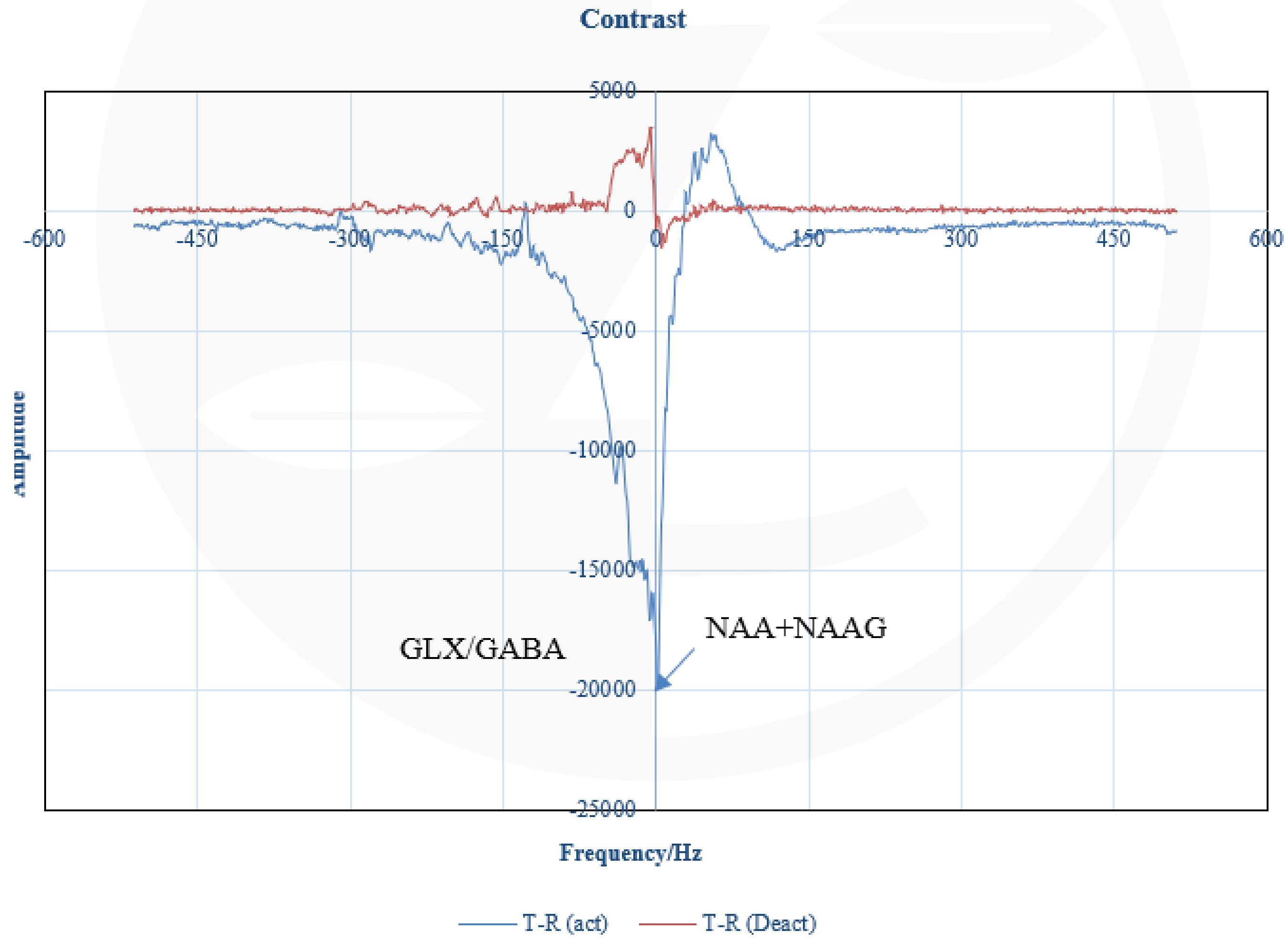

Figure 7. Comparison of the rest-task contrast in the activated (blue) and deactivated (red) brain regions of the Faradarmangars. The regions showing significant differences, along with potential metabolites contributing to these differences, are highlighted with tags.

The change in the spectra obtained from the MRS technique, independent of frequency and based on amplitude, is analyzed in Figure 8. The difference in amplitude comparison independent of frequency shows a significant population difference in the activated brain region, unlike the deactivated region. This observation suggests that different parts of the brain are affected differently by the Faradarmani Consciousness Field. In Taheri's approach, the role of the brain, compared to the mind, is likened to an antenna that receives the processed information from the mind. After receiving this information, it is translated into the language of physics, resulting in metabolic changes and brain activity.

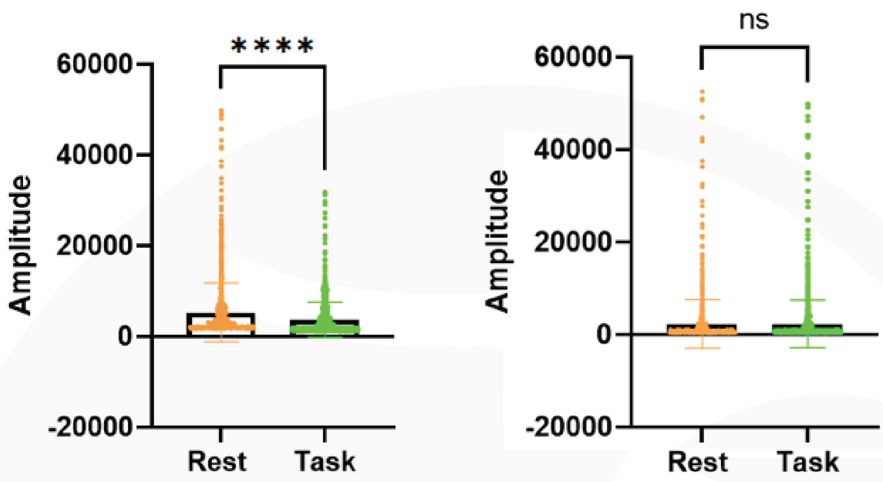

Figure 8. Comparison of the peaks of test and control samples in terms of population amplitudes independent of frequency during paired t-test statistical analysis. Left: Activated brain region. Right: Deactivated brain region. ****: p value < 0.0001.

To better examine the amplitudes within the range produced in this study, as shown in Figure 9, the amplitude values were analyzed in frequency intervals of equal ranges (with 2000-unit intervals).

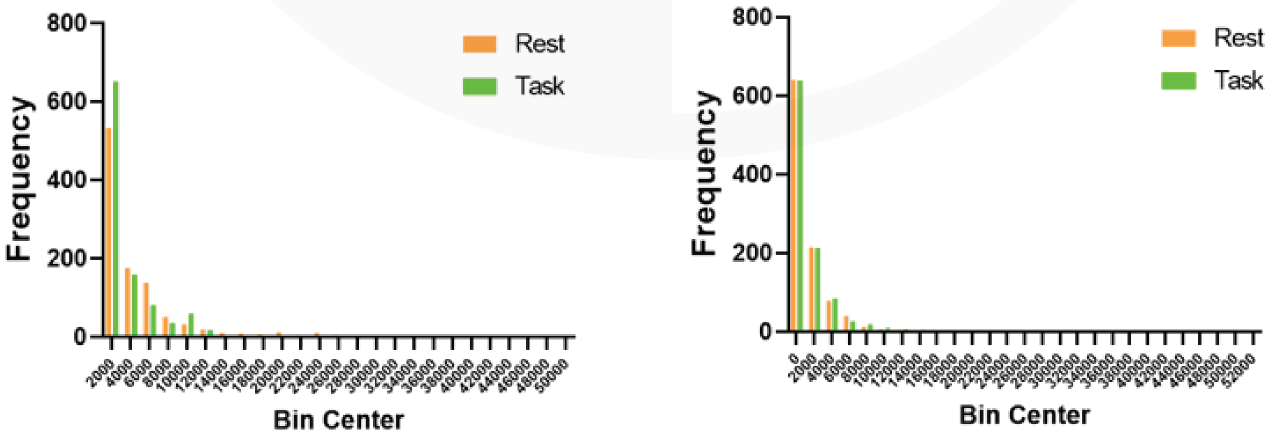

Figure 9. Histogram of amplitude frequency values in the task state (with Faradarmani) and rest state (without Faradarmani) at 2000 intervals. Left: Activated brain region. Right: Deactivated brain region.

In the activated brain region, the difference in the frequency of recorded amplitude values indicates that the effect of the Faradarmani Consciousness Field is associated with an increase in frequency in the first range and a reduction in amplitude values in the terminal ranges (bins between 14000 and 24000). The frequency analysis difference in the deactivated region is not significant. The Shannon entropy calculation based on the frequency analysis data shown in Figure 9 is provided in Table 2.

Table 2. Frequency analysis of amplitude values in different ranges along with the calculation of Shannon entropy.

Activation					Deactivation				
Bin Center	**Rest**	**Task**	**Pi.LnPi (Rest)**	**Pi.LnPi (Task)**	**Bin Center**	**Rest**	**Task**	**Pi.LnPi (Rest)**	**Pi.LnPi (Task)**
2000	533	651	0.339866	0.287967	0	641	639	0.293558	0.294269
4000	176	159	0.30267	0.289207	2000	215	213	0.327599	0.32661
6000	138	81	0.2701	0.200682	4000	78	84	0.196007	0.205132
8000	51	35	0.149396	0.115395	6000	40	26	0.126578	0.093269
10000	32	59	0.108304	0.164436	8000	12	18	0.052069	0.071035
12000	19	17	0.073978	0.068037	10000	6	9	0.030092	0.04161
14000	10	3	0.045204	0.017088	12000	5	6	0.025966	0.030116
16000	8	4	0.037906	0.021661	14000	3	5	0.017075	0.025986
18000	6	3	0.030116	0.017088	16000	4	3	0.021644	0.017088
20000	12	1	0.052108	0.006769	18000	1	2	0.006763	0.012184
22000	5	2	0.025986	0.012184	20000	2	2	0.012174	0.012184
24000	10	2	0.045204	0.012184	22000	2	2	0.012174	0.012184
26000	5	1	0.025986	0.006769	24000	2	2	0.012174	0.012184
28000	3	1	0.017088	0.006769	26000	1	0	0.006763	-
30000	2	2	0.012184	0.012184	28000	2	2	0.012174	0.012184
32000	1	3	0.006769	0.017088	30000	0	0	-	-
34000	2	0	0.012184	-	32000	2	1	0.012174	0.006769
36000	0	0	-	-	34000	0	1	-	0.006769
38000	2	0	0.012184	-	36000	1	1	0.006763	0.006769
40000	0	0	-	-	38000	1	2	0.006763	0.012184
42000	2	0	0.012184	-	40000	0	0	-	-
44000	1	0	0.006769	-	42000	2	1	0.012174	0.006769
46000	2	0	0.012184	-	44000	0	1	-	0.006769
48000	2	0	0.012184	-	46000	0	1	-	0.006769
50000	2	0	0.012184	-	48000	2	1	0.012174	0.006769
Sum	**1024**	**1024**	**1.622741**	**1.255511**	50000	1	2	0.006763	0.012184
					52000	2	0	0.012174	-
					Sum	**1025**	**1024**	**1.221799**	**1.237788**

The calculation of entropy values in the averaged task and rest states in the activated brain region indicates a decrease of approximately 20% in entropy during the task state in the amplitude range of this study. The entropy difference in the deactivated region shows an increase of about 1.3% during the task compared to rest. As mentioned in the introduction, regarding the mechanism of influence of this non-physical field, it is hypothesized that information is transmitted under the influence of the Faradarmani Consciousness Field. The received information leads to observable changes at the brain level. Entropy calculation allows us to infer changes in the content of information. One of the earliest models of information theory is the communication model introduced by Shannon and Weaver (1949). According to this model, a system, prior to receiving information, exists in a physical state characterized by maximum uncertainty and entropy. Upon receiving information, entropy decreases (Shannon and Weaver, 1949; Hoffman et al., 2023). Therefore, before delving into the detailed analysis of metabolite changes, this study provides evidence of the Faradarmani Consciousness Field's influence at the brain level.

In summary, the overall metabolite spectrum analysis indicates a significant and notable decrease in amplitude and entropy of their values as a result of the task in the activated brain region of the Faradarmangars. This metric does not show a significant difference between the test and control in the deactivated region. A detailed analysis of individual metabolites will be presented in subsequent studies.

References

Hoffman, D. D., Prakash, C., & Prentner, R. (2023). Fusions of consciousness. *Entropy, 25*(1), 129. https://doi.org/10.3390/e25010129.

Johnson, K. L., Williams, J. G., Maleki, S. J., Hurlburt, B. K., London, R. E., & Mueller, G. A. (2016). Enhanced Approaches for Identifying Amadori Products: Application to Peanut Allergens. *Journal of agricultural and food chemistry, 64*(6), 1406–1413. https://doi.org/10.1021/acs.jafc.5b05492

Li, J., Zhang, L., Li, H., Ping, Y., Xu, Q., Wang, R., Tan, R., Wang, Z., Liu, B., & Wang, Y. (2019). Integrated entropy-based approach for analyzing exons and introns in DNA sequences. *BMC bioinformatics*, *20*(Suppl 8), 283. https://doi.org/10.1186/s12859-019-2772-y

Liserre, R., Pinelli, L., & Gasparotti, R. (2021). MR spectroscopy in pediatric neuroradiology. *Translational pediatrics*, *10*(4), 1169–1200. https://doi.org/10.21037/tp-20-445

Oz, G., Alger, J. R., Barker, P. B., Bartha, R., Bizzi, A., Boesch, C., Bolan, P. J., Brindle, K. M., Cudalbu, C., Dinçer, A., Dydak, U., Emir, U. E., Frahm, J., González, R. G., Gruber, S., Gruetter, R., Gupta, R. K., Heerschap, A., Henning, A., Hetherington, H. P., … MRS Consensus Group (2014). Clinical proton MR spectroscopy in central nervous system disorders. *Radiology*, *270*(3), 658–679. https://doi.org/10.1148/radiol.13130531

Padelli, F., Mazzi, F., Erbetta, A., Chiapparini, L., Doniselli, F. M., Palermo, S., ... & Cuccarini, V. (2022). In vivo brain MR spectroscopy in gliomas: clinical and pre-clinical chances. *Clinical and Translational imaging*, *10*(5), 495-515. https://doi.org/10.1007/s40336-022-00502-y

Roach, T. N. F. (2020). Use and Abuse of Entropy in Biology: A Case for Caliber. *Entropy (Basel, Switzerland)*, *22*(12), 1335. https://doi.org/10.3390/e22121335

Schmitt, A. O., & Herzel, H. (1997). Estimating the entropy of DNA sequences. *Journal of theoretical biology*, *188*(3), 369–377. https://doi.org/10.1006/jtbi.1997.0493

Shannon, C. E., & Weaver, W. (1949). A mathematical model of communication. *Urbana, IL: University of Illinois Press*, 1-117.

Taheri, MA: "Human from another outlook" Interuniversal Press; 2nd Edition (September 26, 2013). ISBN-13: 978-1939507006, ISBN-10: 1939507006 2013.

Taheri, M. A., Payervand, F., Ahmadkhanlou, F., Torabi, S., & Semsarha, F. (2022a). Investigation of the Influence of Taheri Consciousness Fields on the pH of Pure Water in the Vicinity of Air. *The Scientific Journal of Cosmointel*, *1*(9), 6–33. https://doi.org/10.61450/joci.v1i9.142

Taheri, M. A., Torabi, S., Nabavi, N., Modarresi-Asem, F., Abbasi Sisara, M., Maftoun, P., & Semsarha, F. (2022b). Task-fMRI Group and Functional Connectivity Analysis of the Brain During Faradarmani Consciousness Field Connection. *The Scientific Journal of Cosmointel*, *1*(2), 46–55. https://doi.org/10.61450/joci.v1i2.29

Uda, S. (2020). Application of information theory in systems biology. *Biophysical reviews, 12*(2), 377–384. https://doi.org/10.1007/s12551-020-00665-w

Uda, S., Saito, T. H., Kudo, T., Kokaji, T., Tsuchiya, T., Kubota, H., Komori, Y., Ozaki, Y., & Kuroda, S. (2013). Robustness and compensation of information transmission of signaling pathways. *Science (New York, N.Y.), 341*(6145), 558–561. https://doi.org/10.1126/science.1234511

Vanhamme, L., van den Boogaart A, & Van Huffel S (1997). Improved method for accurate and efficient quantification of MRS data with use of prior knowledge. *Journal of magnetic resonance (San Diego, Calif. : 1997), 129*(1), 35–43. https://doi.org/10.1006/jmre.1997.1244

Wang, L., Whittemore, K., Johnston, S. A., & Stafford, P. (2017). Entropy is a Simple Measure of the Antibody Profile and is an Indicator of Health Status: A Proof of Concept. *Scientific reports, 7*(1), 18060. https://doi.org/10.1038/s41598-017-18469-6

Zambelli, F., Mastropasqua, F., Picardi, E., D'Erchia, A. M., Pesole, G., & Pavesi, G. (2018). RNentropy: an entropy-based tool for the detection of significant variation of gene expression across multiple RNA-Seq experiments. *Nucleic acids research, 46*(8), e46. https://doi.org/10.1093/nar/gky055